Effect of Solder Ball Geometry on Solder Joint Reliability under Solder Reflow Cooling Process

Lau Hong Ming[1], Sujan Debnath[1], Mahzan Johar[1], Siti Faizah Mad Asasaari[2],
Mohd Al Fatihhi Szali Januddi[3], Mohamad Shahrul Effendy Kosnan[3(✉)]
[1]Department of Mechanical Engineering, Faculty of Engineering and Science,
Curtin University Malaysia, Sarawak, Malaysia
[2]School of Mechanical Engineering, Faculty of Engineering,
Universiti Teknologi Malaysia, Johor, Malaysia
[3]Plant Engineering Technology (PETech) Section, Malaysian Institute
of Industrial Technology, Universiti Kuala Lumpur, Johor, Malaysia
mshahruleffendy@unikl.edu.my

Abstract—Solder joint reliability has become an increasingly important factor in electronic industries to obtain sustainable and reliable electronic packages. The simulation study of 3D finite elements on BGA test assembly models with geometries of SMD-NSMD and NSMD-NSMD is conducted through ABAQUS software and is applied with Anand model equation. The applied loading onto the test assembly is set with reflow cooling temperature of 220°C to 25°C. The purpose of this research is to obtain the package warpage, stress, and inelastic equivalent strain throughout the package and solder joints and to develop a predictive finite element model for mechanics and deformation of solder joint in BGA package under reflow cooling. The results obtained showed that solder joints with NSMD-NSMD pad geometry has a greater inelastic equivalent strain and has a greater potential in failing than SMD-NSMD pad geometry. Therefore, it can be concluded that SMD-NSMD pad geometry is more preferable for obtaining a more reliable solder joint.

Keywords—ball grid array, SAC405 solders, reflow cooling, finite element simulation

1   Introduction

With the development of electronic products evolving into better functionality and miniaturization, the size of the solder joints found inside the electronic packaging are also decreasing in size. The purpose of solder joints is to support the electronic package components and act as an electric conductor between the board and components [1]. This development has led to increased concerns about the reliability of the solder joints in electronic packages. There are a few factors that can affect the reliability of solder joints. The IMC layer formed between the solder and the substrate during the solder

reflow process is the factor. An appropriate thickness of the IMC formed is the key for sustaining the reliability of the solder joints. However, IMC is brittle in nature and excessive formation can cause the weakening of joint strength [2]. Another factor that can affect the solder joint's reliability is the equivalent inelastic strain and stress accumulation. As the accumulation of inelastic strain reaches a critical level, fatigue crack of the solder joint is to be expected [3].

Premature solder joint failure is a result mainly caused by the induced stresses that is found in the solder joints. During solder reflow process (SRP), the test assembly with Ball Grid Array (BGA) solders or printed solder paste is exposed to heat with a prescribed temperature profile. This leads to the complete melting of solder, wetting and flowing of molten solder. An intermetallic compound (IMC) layer is developed between the substrate and solder alloy during this process due to chemical reactions from the high reflow temperature. The IMC layer that is developed ensures a good adhesion strength between both the substrate and solder joints. However, as the IMC layer grows to a certain thickness, it can affect the reliability of the electronic package. The IMC layer that has grown too thick can be relatively brittle. With a brittle IMC layer, the solder strength is affected and can possibly cause cracks to occur in the solder joints or in the interface when it is under load [2].

During the process of solder reflow cooling, the temperature used is high. In an electronic package, it compromises of different types of components that are made out of different materials. Unfortunately, different materials have different coefficient of thermal expansion (CTE) values. Due to the differences in the values of CTE, the different materials found in the electronic package will expand and contract at unequal rates [4]. Thus, deformation will occur and potential crack may be formed during the reflow process. Geczy *et al* [5] highlights the temperature in reflow process can be elevated up to a peak temperature of between 208 to 220°C, cracks in the solder joints are tend to occur.

To understand more on the effect of solder reflow process on the reliability of the solder joints with different geometries, FE simulations on two test assemblies with different solder geometries are examined. Different pad geometries of Solder Mask Defined (SMD) and Non-Solder Mask Defined (NSMD) are examined for the FE simulations. Pad designs of SMD and NSMD on the solder joints will be conducted for the first FE simulation and the second simulation will study on pad designs of NSMD and NSMD. By employing FE analysis onto the FE simulations, the accumulated equivalent inelastic strain and von Mises stress can be observed for both cases. With the data obtained from the analysis, the maximum values for stress and strain can be obtained and the optimum configuration for the solder joint geometry can be determined.

2 Finite element modeling

Two cases of FE simulations are performed. The first case is of solder joint with Solder Mask Defined pad design and Non-Solder Mask Defined pad design. The location for the SMD pad at the substrate side while the NSMD pad located at the PCB side. The second case is the solder joints with NSMD and NSMD pad designs, which are located at both substrate and board side. The solder joint with SMD-NSMD and NSMD-NSMD pad design are shown in Figure 1.
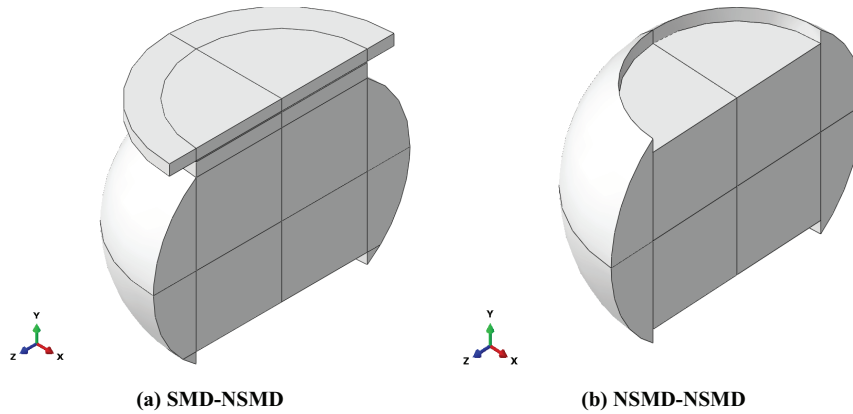
(a) SMD-NSMD   (b) NSMD-NSMD

Fig. 1. Configuration of SAC405 solder ball joint

2.1 Model geometry, loading, boundary conditions and material properties

The design of the model for the BGA test assembly is built based on the dimension from the established work as shown in Figure 2. The components are consisting of silicon die packages which are connected to the FR-4 substrate layer. Then, the substrate layer is connected to the FR-4 PCB through the solder ball. The other components in the test assembly are copper pad and IMC layer. The applied loading for the test assembly is set to be comply with the JEDEC standard for reflow cooling temperature. The temperature set for the test assembly is between 220°C to 25°C.
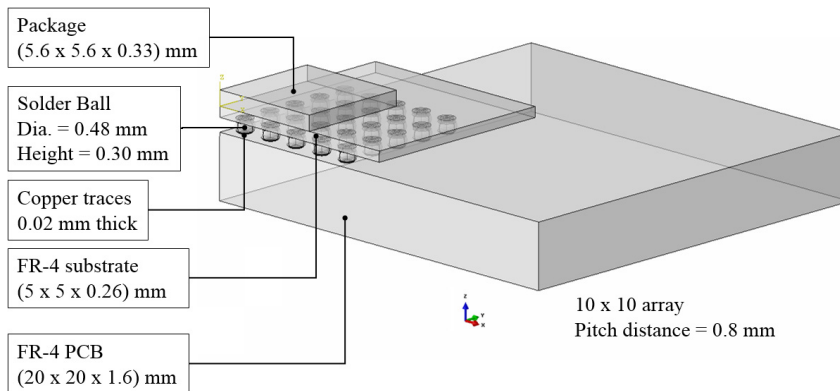

Package
(5.6 x 5.6 x 0.33) mm

Solder Ball
Dia. = 0.48 mm
Height = 0.30 mm

Copper traces
0.02 mm thick

FR-4 substrate
(5 x 5 x 0.26) mm

FR-4 PCB
(20 x 20 x 1.6) mm

10 x 10 array
Pitch distance = 0.8 mm

Fig. 2. Model geometry of BGA test assembly

In this test assembly package, there are a total 100 (10x10) solder ball joints. As for effective simulation, only a quarter model (5x5) of the total test assembly package is considered. The consideration of the employment of quarter model is sufficient for due to symmetry in the model geometry and boundary conditions. Boundary conditions for the BGA assembly are shown in Figure 3. The symmetry boundary conditions are applied to the symmetric plane as mechanical constraints. The displacement and

rotation at the XZ symmetry plane are set to zero in the Y-axis (U_y), rotation about X-axis (UR_x) and Z-axis (UR_z), while the displacement and rotation at the YZ symmetry plane are set to zero in X-axis (U_x), rotation about Y-axis (UR_y) and Z-axis (UR_z). The origin of the Cartesian coordinate axes is fixed using a material point to avoid rigid body movement.
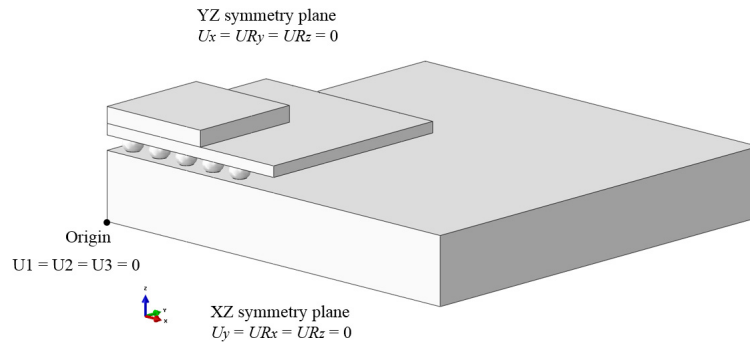

Fig. 3. A quarter model of BGA test assembly

The material properties such as SAC405 solder, silicon die package, copper layer and substrate are dependent on temperature. Hence, the elastic modulus of those materials is defined as in the Table 1.

Table 1. Various materials in BGA assembly model used in FE simulation

Material	E (GPa)	v	CTE (ppm/^{o}C)
Sn4.0Ag0.5Cu [6, 7]	$44.7 - 0.146\,T$ (^{o}C)	0.36	20
Si-die [8]	$132.46 - 0.00954\,T$ (K)	0.28	$2.113 + 0.00235\,T$(K)
Copper layer [8]	$141.92 - 0.0442\,T$ (K)	0.35	$15.64 + 0.0041\,T$(K)
Cu$_6$Sn$_5$ [9]	85.6	0.31	16
FR-4 PCB & Substrate (isotropic in xy-plane) [10]			
E_x & E_y (MPa)	G_{xy} (MPa)	v_{xy}	α_x and α_y (ppm/$^{\circ}$C)
$27,924 - 37$ T(K)	$12,600 - 16.7$ T(K)	0.11	16
E_z (MPa)	G_{xz} and G_{yz} (MPa)	v_{yz} and v_{xz}	α_z (ppm/$^{\circ}$C)
$12,204 - 16$ T(K)	$5,500 - 7.3$ T(K)	0.39	84

3 Results and discussion

Results of the finite element simulation of two different types of solder geometry are presented and discussed in terms of results of the package warpage as well as the stress and equivalent inelastic strain distribution which is located throughout the package and critical solder joint

Package warpage: As the BGA solder joints undergo reflow cooling process, the test assembly is exposed to a change in temperature from the reflow temperature of 220°C to the ambient temperature of 25°C. Due to the temperature difference between the assembly and the surroundings and different materials have different coefficients of thermal expansion (CTE) value, mismatches in the CTE occur in assembly. The SAC 405 solder, silicon die, Cu pad, FR-4 PCB and FR-4 substrate has CTE values of 20 ppm/°C, 2.113 ppm/K, 15.64 ppm/K, 16 ppm/°C and 84 ppm/°C respectively. Thus, this induces thermal strains and stresses to be developed. Previous studies have reported that an increase in CTE mismatches has a linear correlation with the increment of tensile stress and compressive stress. It has been conclusively shown that compressive stress increases faster than tensile stress during a positive CTE mismatch. On the other hand, a negative CTE mismatch leads tensile stress to increase faster than compressive stress [11].

Figure 4a shows the FE simulation results of the quarter model test assembly at 25°C with the predicted warpage in the vertical direction of the y-axis. The warpage of the quarter model obtained from the simulation shows a value of 0.04764 mm. The predicted deformation of the quarter model shows a convex shape due to the greater CTE value of the FR-4 PCB. The substrate and the FR-4 PCB found in the assembly have a CTE value of 84 and 16 ppm/°C, while the silicon dies CTE value of 2.113 ppm/°K. As the FR-4 PCB and substrate have a higher CTE value, the two components cause a positive difference in CTE values against the silicon die. Thus, this promotes expansion differences between the two components. Previous studies have reported that a greater differences in CTE values resulted in a sizeable deformation [12]. As the different components found in the quarter model remain bonded together throughout the process, deformation occurs due to the different contraction where the PCB and substrate pull the silicon die. The FR-4 PCB and substrate will have a greater contraction which causes greater compressive stress when compared to the silicon die. Thus, this promotes the deformation of the assembly to occur into a dome-like shape with a smooth downward deflection. Our finding revealed that the obtained results are consistent with the study by Liao *et al* [13], which successfully described the thermally-induced deformation of PCB assembly.

In comparison to the results obtained from the SMD-NSMD FE simulation, which shows a deformation of 0.04764 mm, results obtained from this simulation concludes that the deformation that occurs on the NSMD-NSMD as shown in Figure 4b test assembly is greater than the SMD-NSMD test assembly. The greater deformation found in the NSMD-NSMD quarter model test assembly is due to the pad shape of the solder joints.
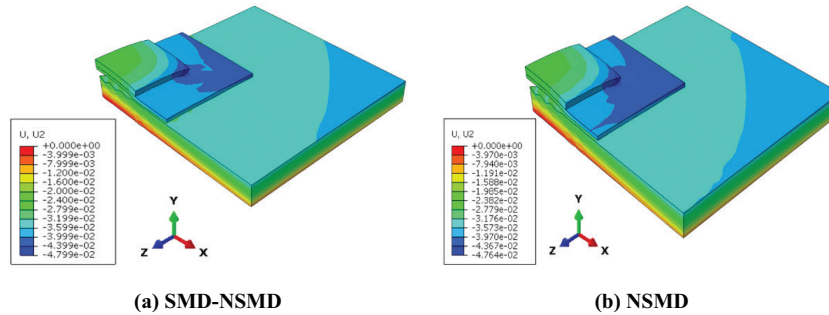
(a) SMD-NSMD   (b) NSMD

Fig. 4. FE simulation results for deformation of the quarter model test assembly

***Stress distribution*:** Figure 5 shows the FE simulation of the von Mises stress distribution throughout the solder balls in the quarter model test assembly ball for the SMD-NSMD and NSMD-NSMD. The simulation results obtained indicates that all of the solder balls experience stress after undergoing solder reflow process. However, some solder balls experience more stress when compared to the others. Previous research conducted by Zhao *et al* [14] shown that the maximum stress of the solder joint occurs at the edges of the connection with the substrate and PCB. Similarly, the results obtained from the FE simulation shows a greater stress concentration located at the edges of the substrate and PCB.

The solder ball D4, which experiences the greatest amount of stress, is the critical solder ball. The critical solder ball is the focus of the analysis as it is the most likely to cause the failure of the package. The critical solder ball allows the indication of potential fatigue failure sites.
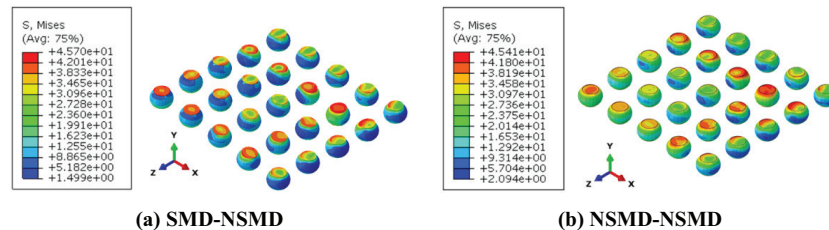

(a) SMD-NSMD   (b) NSMD-NSMD

Fig. 5. Von Mises Stress distribution throughout the solder balls

Figure 6 shows the result of the FE simulation on the von Mises Stress distribution throughout the bottom part of the critical solder ball for the SMD-NSMD and NSMD-NSMD. The geometrical shape of the top of the solder is SMD pad design while the bottom is NSMD pad design as shown in Figure 6b. The highest concentration of stress is located at the edge and the bottom part of the solder ball. The bottom part experiences a maximum stress of magnitude 45.7 MPa. The NSMD pad shows that the stress concentration is distributed unevenly, and some parts do not experience a high concentration of stress. Meanwhile, the top part experiences stress throughout the area and shows the stress is distributed throughout the whole top area. The stress built up in the solder ball is due to the severe CTE mismatches between the materials solder

ball and the PCB/substrate [14]. Not only that, but the critical solder ball is also compressed between the PCB and substrate. The NSMD pad of the solder ball has sharp edges inside the pad and is being compressed by the PCB. Due to the pad design, the maximum stress is observed to be located at the bottom. As the accumulation of stress in the solder ball reaches a magnitude such that plastic relaxation could not release it. Cracks will be formed at the highest stress area, which leads to local recrystallization that affects the crack propagation [15].

The maximum stress that is experienced by the NSMD-NSMD that went through solder reflow process is at a magnitude of 45.41 MPa as shown in Figure 6b. Both the top and the bottom side of the critical solder joint is in the shape of NSMD. The maximum stress is located at the bottom edge of the solder joint. The distribution of stress on the internal top part of the solder is more consistent when compared to the bottom part. The stress distribution at the top is more widely spread, while the bottom part shows an inconsistent stress distribution throughout the whole surface. The bottom stress distribution also shows that the stress is located at a certain point while spreading inwards rather than just on the surface of the NSMD pad.
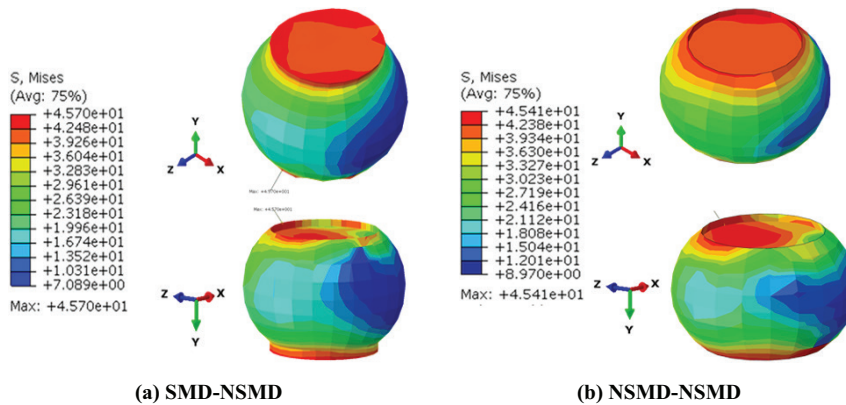

(a) SMD-NSMD (b) NSMD-NSMD

Fig. 6. Von Mises Stress distribution of the critical solder ball

When compared to the SMD-NSMD test assembly, the location of the stress in this simulation is similar to the SMD-NSMD test assembly, which is at the bottom of the joint, facing the PCB side. The maximum stress which is located at the bottom of the solder joint is due to the geometrical shape of the NSMD pad. The results shows that the NSMD-NSMD test assembly has a slightly lesser value in stress. Not only that, as the CTE value of FR-4 substrate is greater than the CTE value of FR-4 PCB, this causes a greater expansion for the substrate than the PCB. Therefore, the pad located at the bottom of the solder experiences more stress.

Equivalent Inelastic Strain (CEEQ): In this simulation, the unified model is used to assume the creep deformation and plasticity can be integrated with elastic deformation and can be directly calculated. The CEEQ is governed by the Anand constitutive model, used to represent the material behavior of solder in finite element simulations.

Figure 7 shows the FE simulation of the cross-sectional part of the quarter model test assembly with the internal strain distribution for the SMD-NSMD and NSMD-NSMD. It

is apparent that the strain shown in Figure 7a shows a small concentration throughout the whole test assembly. However, a significant amount of strain is located at a certain solder joint in the test assembly, which is known as the critical solder joint. The critical solder joint with a maximum CEEQ value of 0.01237 is analyzed as it has the most significant amount of strain and has the highest potential in leading to failure. Identical location of the critical solder was observed for NSMD-NSMD as shown in Figure 7b, the maximum CEEQ that is experienced by the critical solder joint shows a value of 0.01837.
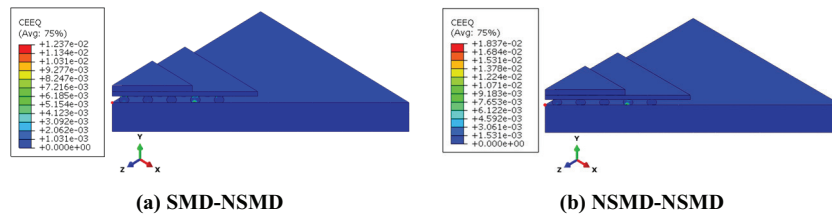

(a) SMD-NSMD   (b) NSMD-NSMD

Fig. 7. CEEQ Solder Diagonal Cut for SMD-NSMD test assembly

Figure 8 illustrates the top part and the bottom part of the critical solder ball in the test assembly with its predicted characteristics. The solder ball is stated to be in the geometrical pad shape of Solder Mask Defined (SMD) at the top part while being Non-Solder Mask Defined at the bottom part. The maximum value of the CEEQ found in the critical solder ball is 0.01237. At the top part of the solder ball, the concentration of the inelastic strain is confined and concentrated to a small circular region around the edge. At the same time, it slowly fades and declines to the center of the solder ball, where it remains elastic. The finding obtained from the simulation shows a similar result to those obtained by Yamin *et al* [16]. As for the bottom part, the NSMD pad experiences lesser inelastic strain throughout the whole surface than the SMD pad. However, the result shows that the maximum inelastic strain is located at the NSMD pad.
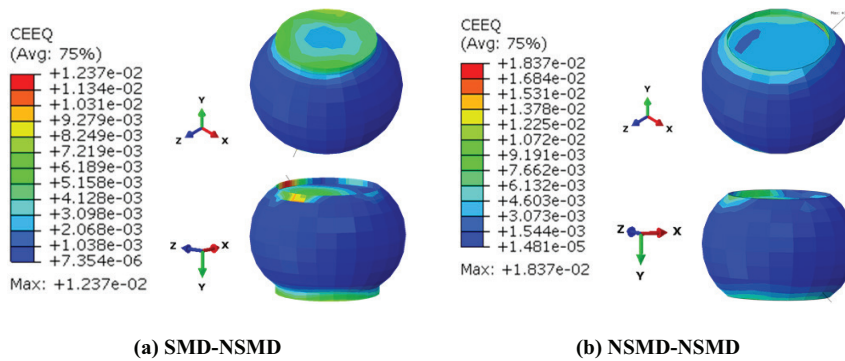

(a) SMD-NSMD   (b) NSMD-NSMD

Fig. 8. CEEQ distribution of the top part of the Critical Solder Ball

The test assembly had undergone solder reflow cooling process which promotes the fatigue characteristics found in the solder joint. The primary strain that can be found in the accumulated inelastic strain is the creep strain component. Throughout the process of reflow cooling, the inelastic strain accumulates relative to the stress applied to the

yield surface. Studies were conducted in determining how the cooling rate of the solder affects the magnitude of stress and strains [17]. At a higher straining rate, the intrinsic hardening rate of the alloy will also be higher. Thus, this will lead to a greater cooling rate which produces a greater inelastic strain. When solder is exposed to a longer cooling period, solder joints subjected to the high temperatures will eventually lead to a greater thickness in the formation of inter-metallic compound (IMC) and more inelastic strain in the solder joint. Nucleation process which promotes the IMC formation is favored at a longer cooling rate. The finding is consistent with the findings of past studies which was conducted by [18], which indicates IMC formation to be greater at a higher cooling rate. However, in contrary to the findings which revealed SMD pads are more susceptible to failure, the results obtained from the FE simulation for SMD-NSMD test assembly shows that the maximum CEEQ value is located at the NSMD pad. Thus, the NSMD pad can be stated to be more susceptible to failure.

When compared to the SMD-NSMD test assembly, the CEEQ value for the NSMD-NSMD test assembly has a greater value. The distribution of the inelastic strain is uneven for both the top side and bottom side when compared to the SMD-NSMD test assembly. The top side of the solder joint contributes to the greater value of strain as the NSMD pad has sharp edges. [19] researched the strain rate on the stress-strain response of solder alloys. The author discovered that a higher strain rate leads to the increment in the strength of solder alloys. However, the higher strain level also leads to an accelerated fatigue failure of solder joints at roughly 60 – 83% of lifetime reduction. From the data obtained from the simulation, it is apparent that the NSMD-NSMD test assembly has a greater strength as compared to the SMD-NSMD test assembly. However, the NSMD-NSMD test assembly will also potentially reach failure faster than the SMD-NSMD test assembly.

Comparison between von Mises and CEEQ: The CEEQ in SMD-NSMD test assembly illustrates that the maximum strain is at the bottom of the joint. However, for NSMD-NSMD test assembly, the maximum strain is located at the top of the solder joint. According to the Table 2, NSMD-NSMD test assembly shows a greater CEEQ value. The greater CEEQ value can lead to a greater accumulation of IMCs in future subsequent temperature cycles and accelerate failure process. The greater value of CEEQ shown in the NSMD-NSMD test assembly is due to its geometrical pad shape. The pad design consists of sharp internal edges for both top and bottom of the solder joints which causes the NSMD pad design to be compressed by the PCB and substrate. With the compression, it leads to the greater strain value.

Table 2. Data comparison between test assemblies

	Package Deformation (mm)	Yield Strength (MPa)	Equivalent Inelastic Strain	von Mises Stress (MPa)
SMD-NSMD	0.04764	623.9	0.01237	45.70
NSMD-NSMD	0.04799	642.0	0.01837	45.41

However, the stress value found in the simulation for the test assemblies does not show a greater value for the NSMD-NSMD model. Not only that, the stresses for both the test assemblies are shown to be located at the bottom of the solder joint, facing the PCB side. The thermal and mechanical stress can cause a weaken coarsened structure

in the solder joint which leads to the accelerated formation of brittle IMCs. In contrary to the findings of Lee *et al* [20] which showed that NSMD pad design is preferred over SMD design, the results obtained from the FE simulation shows that SMD is more preferable in this study due to a lower CEEQ value.

4   Conclusion

According to the analysis shown, the NSMD-NSMD solder joint is known to have a 48.5% greater equivalent inelastic strain than the SMD-NSMD solder joint. However, the von Mises stress accumulation for NSMD-NSMD solder joint is only 0.63%. Thus, during subsequent temperature cycles, the solder joints with NSMD-NSMD geometry have a greater potential of reaching failure due to the accumulation of strain that leads to the increasing build up of IMC layer.

5   References

[1] Wang S, Yao Y, Long X. Critical review of size effects on microstructure and mechanical properties of solder joints for electronic packaging. Applied Sciences. 2019;9(2):227. https://doi.org/10.3390/app9020227

[2] Li Z, Li G, Li B, Cheng L, Huang J, Tang Y. Size effect on IMC growth in micro-scale Sn-3.0 Ag-0.5 Cu-0.1 TiO2 solder joints in reflow process. Journal of Alloys and Compounds. 2016;685:983–91. https://doi.org/10.1016/j.jallcom.2016.06.295

[3] Zhao C, Shen C, Hai Z, Zhang J, Bozack M, Evans J, editors. Long term aging effects on the reliability of lead free solder joints in ball grid array packages with various pitch sizes and ball alignments. SMTA International; 2015.

[4] Ogbomo OO, Amalu EH, Ekere N, Olagbegi P. Effect of coefficient of thermal expansion (CTE) mismatch of solder joint materials in photovoltaic (PV) modules operating in elevated temperature climate on the joint's damage. Procedia Manufacturing. 2017;11:1145–52. https://doi.org/10.1016/j.promfg.2017.07.236

[5] Illés B, Krammer O, Geczy A. Reflow Soldering: Apparatus and Heat Transfer Processes: Elsevier; 2020. https://doi.org/10.1016/B978-0-12-818505-6.00002-9

[6] Qiang W, Lihua L, Xuefan C, Xiaohong W, Liu Y, Irving S, et al., editors. Experimental Determination and Modification of Anand Model Constants for Pb-Free Material 95.5Sn4. OAgO.5Cu. International Conference on Thermal, Mechanical and Multi-Physics Simulation Experiments in Microelectronics and Micro Systems EuroSime 2007; 2007. https://doi.org/10.1109/ESIME.2007.359957

[7] Schubert A, Dudek A, Auerswald E, Gollhardt A, Michel B, Reichl H. Fatigue Life Models for SnAgCu and SnPb Solder Joints Evaluated by Experiments and Simulation. Proceedings of the 2003 Electronic Components and Technology Conference. 2003:603–10. https://doi.org/10.1109/ECTC.2003.1216343

[8] Shi XQ, Wang ZP, Zhou W, Pang JHL, Yang QJ. A new creep constitutive model for eutectic solder alloy. ASME Journal of Electronic Packaging. 2002;124(2):85–90.

[9] Amagai M. Chip scale package (CSP) solder joint reliability and modeling. Microelectronics Reliability. 1999;39(4):463–77. https://doi.org/10.1016/S0026-2714(99)00017-7

[10] Zahn BA, editor. Solder joint fatigue life model methodology for 63Sn37Pb and 95.5Sn4Ag0.5Cu materials. Electronic Components and Technology Conference, 2003 Proceedings 53rd; 2003.

[11] Jikihara AN, Tanaka CB, Ballester RY, Swain MV, Versluis A, Meira JB. Why a zero CTE mismatch may be better for veneered Y-TZP structures. Journal of the Mechanical Behavior of Biomedical Materials. 2019;96:261–8. https://doi.org/10.1016/j.jmbbm.2019.04.049

[12] Huang C-Y, Ying K-C. Applying strain gauges to measuring thermal warpage of printed circuit boards. Measurement. 2017;110:239–48. https://doi.org/10.1016/j.measurement.2017.06.029

[13] Liao M-C, Huang P-S, Lin Y-H, Tsai M-Y, Huang C-Y, Huang T-C. Measurements of thermally-induced curvatures and warpages of printed circuit board during a solder reflow process using strain gauges. Applied Sciences. 2017;7(7):739. https://doi.org/10.3390/app7070739

[14] Zhao S-J, Huang C-Y, Tang X-Q, Lu L-K, editors. Simulation Analysis of Residual Stress of BGA Solder Joints After Reflow Soldering Based on Element Birth and Death Technology, (ICEPT); 2018: IEEE. https://doi.org/10.1109/ICEPT.2018.8480531

[15] Gao L-Y, Liu Z-Q, Li C-F. Failure mechanisms of SAC/Fe-Ni solder joints during thermal cycling. Journal of Electronic Materials. 2017;46(8):5338–48. https://doi.org/10.1007/s11664-017-5554-1

[16] Yamin A, Abdullah A, Manap M, Yusoff H, editors. Failure prediction of the solder joints in the ball-grid-array package under thermal loading. Journal of Physics: Conference Series; 2019: IOP Publishing. https://doi.org/10.1088/1742-6596/1349/1/012013

[17] Hu X, Xu T, Jiang X, Li Y, Liu Y, Min Z. Effects of post-reflow cooling rate and thermal aging on growth behavior of interfacial intermetallic compound between SAC305 solder and Cu substrate. Applied Physics A. 2016;122(4):278. https://doi.org/10.1007/s00339-016-9893-1

[18] Yang L, Ge J, Liu H, Xu L, Bo A. Effect of Cooling Rate on the Microstructure and Mechanical Properties of Sn-1.0 Ag-0.5 Cu–0.2 BaTiO 3 Composite Solder. Journal of Electronic Materials. 2015;44(11):4595–603. https://doi.org/10.1007/s11664-015-3993-0

[19] Dalton E, Ren G, Punch J, Collins MN. Accelerated temperature cycling induced strain and failure behaviour for BGA assemblies of third generation high Ag content Pb-free solder alloys. Materials & Design. 2018;154:184–91. https://doi.org/10.1016/j.matdes.2018.05.030

[20] Lee T-K, Chen Z, Guirguis C, Akinade K. Impact of isothermal aging and testing temperature on large flip-chip BGA interconnect mechanical shock performance. Journal of Electronic Materials. 2017;46(10):6224–33. https://doi.org/10.1007/s11664-017-5650-2

6   Authors

Lau Hong Ming, Department of Mechanical Engineering, Faculty of Engineering and Science, Curtin University Malaysia.

Sujan Debnath, Department of Mechanical Engineering, Faculty of Engineering and Science, Curtin University Malaysia.

Mahzan Johar, Department of Mechanical Engineering, Faculty of Engineering and Science, Curtin University Malaysia.

Siti Faizah Mad Asasaari, School of Mechanical Engineering, Faculty of Engineering, Universiti Teknologi Malaysia.

Mohd Al Fatihhi Szali Januddi, Advanced Facilities Engineering Technology Research Cluster (AFET), Plant Engineering Technology (PETech) Section, Malaysian Institute of Industrial Technology, Universiti Kuala Lumpur, 81750 Masai, Johor, Malaysia.

Mohamad Shahrul Effendy Kosnan, Advanced Facilities Engineering Technology Research Cluster (AFET), Plant Engineering Technology (PETech) Section, Malaysian Institute of Industrial Technology, Universiti Kuala Lumpur, 81750 Masai, Johor, Malaysia.